Convective Boundary Layer Height Measurement with Wind Profilers and Comparison to Cloud Base

ALISON W. GRIMSDELL AND WAYNE M. ANGEVINE

CIRES, University of Colorado, and NOAA Aeronomy Laboratory, Boulder, Colorado

(Manuscript received 29 September 1997, in final form 20 January 1998)

ABSTRACT

The depth of the atmospheric boundary layer is of interest in several different areas, such as chemistry, pollutant studies, and global modeling. In this research the authors describe and compare several different measurements of boundary layer depth. First, the authors use the standard measurement from radiosondes to confirm the validity of wind-profiler measurements, which use humidity gradients to estimate the boundary layer depth. A method for obtaining meaningful cloud-base altitudes is then presented, and the results are compared to the wind-profiler boundary layer heights. The authors find good agreement between the different types of measurement but see that the profiler peak reflectivity is slightly raised above cloud base in the presence of boundary layer clouds. This may be due to increased humidity gradients at the top and edges of clouds or to increased turbulence within the cloud. Calculation of the boundary layer height using the bulk Richardson number is commonly used in computer models. Comparison with the authors' profiler measurements indicates that the calculation overestimates the height of the boundary layer and that the agreement between the methods is poor.

1. Introduction

A better understanding of the structure and behavior of the atmospheric boundary layer is required for understanding and modeling of the chemistry and dynamics of the atmosphere on all scales. In this paper we investigate one of the most basic boundary layer properties: the depth of the layer. The type of boundary layer of interest in this study is a continental convective boundary layer (CBL). The general characteristics of the diurnal cycle are fairly well known, as described, for example, by Grossman and Gamage (1995) and Stull (1988).

Precise measurements of the CBL height (also known as the ''mixing height'') are of special importance to local and regional air pollution studies because the CBL height governs the concentration of surface-emitted species. Changes of CBL height with time can also result in entrainment of elevated layers of pollutants and thus can change the pollutant concentrations in the CBL and at the ground (e.g., Trainer et al. 1995). CBL height measurements with boundary layer wind profilers are now a common part of many field campaigns addressing air quality: for example, the 1992 Rural Oxidants in the Southern Environment II Campaign (Angevine et al. 1994), the 1995 Southern Oxidants Study (White 1997), and the Montreal Experiment on Regional Mixing and Ozone (Donaldson et al. 1997). CBL height is a basic scaling parameter for fluxes and variances, and therefore, CBL height measurements are a key part of experiments designed to elucidate basic boundary layer structure and behavior, such as the Flatland95, Flatland96, and Flatland97 experiments, as well as the continuous operations at the Flatland Atmospheric Observatory (Angevine et al. 1998). Profilers are also used to estimate mixing heights in marine boundary layers (White et al. 1991). Many other field experiments have used radiosonde estimates of the CBL height [several are listed in Stull (1988)]. Cloudy boundary layers are particularly poorly understood. In all cases, there is a need for reliable measurements to test and improve the representation of CBL height in numerical models at all scales.

The CBL height can be detected by boundary layer wind profilers (see section 2) as an enhancement in the radar reflectivity due to strong humidity gradients and turbulence (White et al. 1991). The most basic form of the data is shown in Figs. 1 and 2, in which the uncalibrated reflectivity is plotted in pseudocolor (grayscale) for every vertical beam (roughly every 100 s). The boundary layer top is clearly visible as a strong enhancement in the reflectivity. The values of CBL height z_i determined by an automated algorithm (Angevine et al. 1994) for hour averages every half hour are shown as a solid line. The algorithm simply finds the height of peak reflectivity in each 25-s sample and then takes the median of those heights over an hour as

Corresponding author address: Alison W. Grimsdell, NOAA, R/E/AL3, 325 Broadway, Boulder, CO 80303.

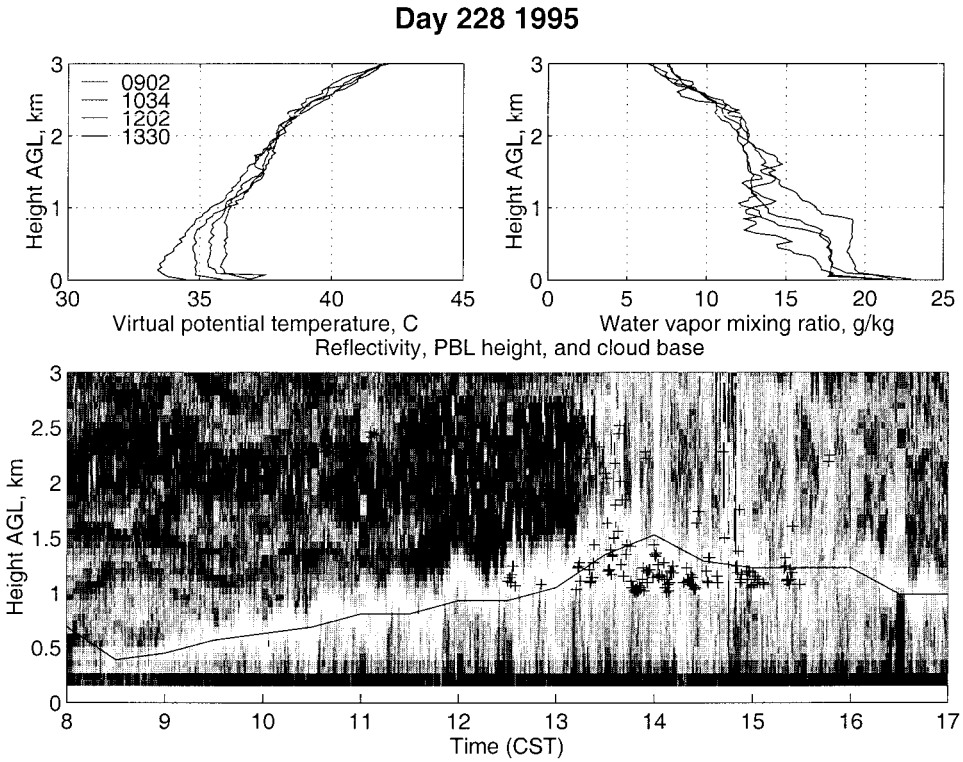

FIG. 1. Boundary layer development for day 228 (16 August) 1995. Upper plots show radiosonde profiles of virtual potential temperature (left) and water vapor mixing ratio (right) at different times during the day as the depth of the mixed layer increases. The lower plot shows the profiler peak reflectivity as a grayscale. Lighter shades indicate a stronger return, with the algorithm-selected height for the hour shown by a solid line. The ceilometer cloud measurements are indicated by crosses.

z_i. Cloud heights found by a laser ceilometer sampling every 30 s are shown as crosses. Four radiosonde soundings are also plotted for each day, which can be distinguished by the expected diurnal evolution of CBL height and temperature. Day 228 (16 August) 1995 (Fig. 1) was warm and humid. The capping inversion was relatively weak, and the lower free troposphere was also humid. Day 219 (6 August) 1996 (Fig. 2) was also warm and humid, but the capping inversion was much stronger and the free troposphere was much drier.

Figures 1 and 2 show clearly that the profiler can measure z_i in well-defined convective boundary layers; the figures illustrate several other points as well. When a cloud layer of significant depth is present at the CBL top, after 1300 CST on day 228, for example, the reflectivity gradient is poorly defined or displaced to a cloud top or cloud edge, and z_i is difficult to determine. In fact, the definition of z_i in this case is ambiguous and needs further discussion. So this is more a limitation of our understanding than of our instruments. Shallow CBL–top clouds as on day 219 do not have such a strong effect. Other interesting phenomena are also visible in these plots. For example, the capping inversion above a residual layer is visible at approximately 1.3 km from 0800 CST until just after 1000 CST on day 219, and several humidity layers are visible above the CBL in the morning of day 228 between 0800 and 1130 CST. The boundary layer evolution is clearly very different on the two days. On day 228, the CBL grows slowly, and we see a quasi-periodic structure in the CBL top until the clouds form. On day 219, the CBL grows quickly into the residual layer and then grows more slowly after reaching the capping inversion. In both cases, the entrainment zone has significant depth on both short (a few minutes) and long (hour) scales, as indicated by both the width of the region of high profiler reflectivity and the shape of the radiosonde profiles. Downdrafts entraining air from above the CBL and therefore moving the humidity gradient downward are clearly visible, at around 1130 and 1315 CST on day 219, for example. Some of the visible structure may also be due to contamination (e.g., by insects), but none is clearly identifiable on these two days. Much of the signal in the middle of the boundary layer may be due to insects rather than to clear-air refractive index fluctuations (Clark et al. 1995), but the CBL–top cloud structure seems to be primarily due to clear-air scattering. These phenomena require some effort in understanding their effect on the measurement and subsequent data quality controls.

Angevine et al. (1994) and others have shown cases of profiler measurements of convective boundary layer

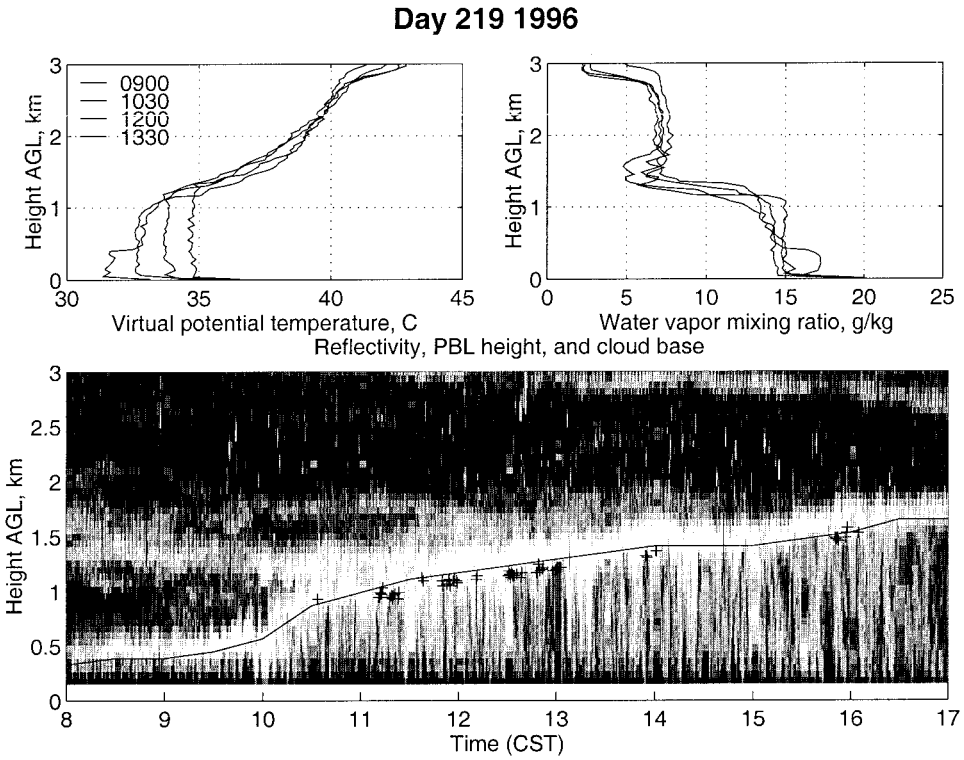

FIG. 2. As for Fig. 1 but showing the boundary layer development on day 219 (6 August 1996).

heights, but here we present statistics of a much larger dataset. Data from field campaigns operated during August–September 1995 and June–August 1996 are examined and interpreted in the context of the standard model for boundary layer development. The effect of clouds is of special interest and is examined in more detail.

2. Experiment layout and instrumentation

The Flatland experiments are described by Angevine et al. (1998). Three sites were established, forming a triangle with sides of 5.7, 7.5, and 7.6 km. A 915-MHz Doppler wind profiler, and a surface station were located at each of the three sites. The Flatland Atmospheric Observatory (FAO) site also recorded up to three vertical layers of cloud using a ceilometer. Radiosondes were launched at least daily—occasionally four times a day—from the Sadorus site, located about 7 km southwest of FAO at the southwest vertex of the triangle. The study area is southwest of Champaign–Urbana, Illinois, and the surrounding land is extremely flat and planted with approximately equal amounts of soybeans and corn.

The 915-MHz lower-troposphere (boundary layer) wind profiler was developed at the National Oceanic and Atmospheric Administration (NOAA) Aeronomy Laboratory (Carter et al. 1995; Ecklund et al. 1988). These transportable systems have been deployed at the sites of many meteorological and atmospheric chemistry experiments, as well as at the sites of long-term studies in the Tropics. The wind profilers are sensitive Doppler radars, designed to respond to refractive index fluctuations in clear air. In the boundary layer, the major influence on the refractive index is humidity. The strong return observed at the top of the boundary layer is due to the humidity gradient from the humid lower-layer air to the drier air of the free troposphere (White et al. 1991). Since hydrometeors, birds, aircraft, and insects also produce a strong return, we have excluded days with noticeable rainfall and have used processing software that includes an intermittent contamination removal algorithm (the so-called bird algorithm) (Merritt 1995) to remove the effect of contamination from a variety of objects, particularly birds.

For the Flatland experiments, the profilers operated at 60-m vertical resolution with a minimum height of 150 m AGL. Six beam positions—four oblique beams in two coplanar pairs and two vertical beams of orthogonal polarization—were used. The dwell time on each beam was approximately 25 s.

A Vaisala RS80-15LH radiosonde was launched each day at 1200 CST, providing profiles of temperature and humidity, as well as wind speed and direction. On some days, when a well-developed boundary layer was expected to form, four radiosondes were launched 1.5 h apart from 0900 to 1330 CST to capture better the boundary layer evolution.

The Vaisala CT25K ceilometer is a vertically pointing laser device operating at 905 nm. It records the intensity of the return from the atmosphere and can infer the presence of up to three cloud layers. The ceilometer does not specifically measure cloud base but instead receives a strong return when any part of a cloud is directly above it. In some cases it also records ''obscuration,'' in which case the return was higher than for a clear atmosphere, but no specific cloud altitude could be determined. Hazy conditions giving rise to this reading were not uncommon. Ceilometer data selection for the comparisons is discussed in section 5. The ceilometer was located at FAO.

Surface measurements are used to calculate the lifting condensation level (LCL). This is the altitude at which surface air would reach saturation (and form clouds) if it were to be raised adiabatically. Due to surface inhomogeneities and entrainment processes, the calculated LCL is not usually exactly the same as the cloud base but should be similar under the conditions of this experiment. Surface data were averaged over the hour of interest for comparison with other measurements.

3. Profiler data processing

The focus of this research is to investigate well-defined continental convective boundary layers. To this end, we want to remove hours when these conditions are not present—for example, there may be fog, rain, or stratus cloud reducing the surface heating. Profiler data were selected using an intersite comparison method that incorporates data from all three profilers; comparable results can be achieved with a single profiler and careful manual quality control.

Hourly values of boundary layer height for each profiler were found using an automatic algorithm (Angevine et al. 1994). The peak reflectivity of each vertical beam measurement during the hour was found, and the overall boundary layer height for that hour was taken as the median of these peaks. The standard deviation of the peak heights was used as a measure of how well formed the boundary layer was during the hour.

For each hour we subjectively inspected the boundary layer estimate from each profiler and produced an average boundary layer height and an indication of the reliability of the result. Results were discarded if rain was present during the hour, if the signal had poor spatial or temporal coherence, or if the boundary layer height estimate was below 270 m—the lower limit due to hardware limitations—or above 3000 m, which is unrealistically high.

4. Comparison with radiosonde data

The boundary layer height z_i measured by the radiosondes was determined subjectively from each profile. A confidence level was also assigned subjectively based on how well the profile fit our conceptual model of the typical boundary layer structure (e.g., Stull 1988, 12). Figure 3 compares the profiler and radiosonde estimates of z_i for both years of the campaign. The radiosonde data include points with a confidence level in one of the best three (of four) categories, and the profiler data, selected as described in the previous section, is for the hour corresponding to that of the radiosonde launch.

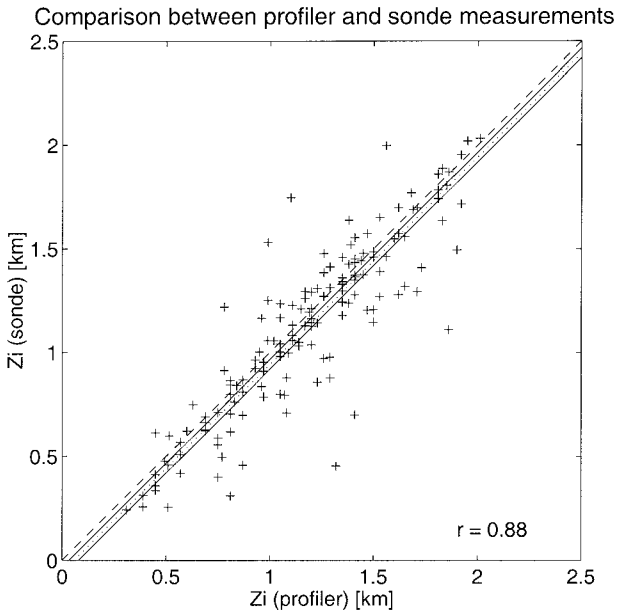

FIG. 3. Boundary layer depth as determined by radiosonde compared to profiler peak reflectivity. The mean z_i from the profiler = 1181 m, the mean z_i from the radiosonde = 1125 m, and the correlation coefficient is 0.88 from 150 points. The dashed line is 1:1, the dotted line shows the mean difference, and the two solid lines are at the mean difference plus and minus the standard deviation of the mean difference.

Figure 3 shows generally very good agreement between the two measurement techniques, with a slight bias toward higher z_i measured by the profiler. There seemed to be a stronger bias when clouds were present, so the data were stratified using this criterion, as shown in Fig. 4. From this figure we see that both the bias and scatter are larger in cloudy conditions. Using the standard deviation of the mean difference, σ_{md}, as an indicator of the significance of the bias, we calculate for clear conditions a bias of 39 m and a σ_{md} of 15 m, while for cloudy conditions we see a bias of 71 m and a σ_{md} of 27 m. This indicates that although the bias is small in both cases, it is more significant in the cloudy case. Note that the size of the radar range gate is 60 m, so that in the clear case the bias is less than the resolution of the measurements, while in the cloudy case the bias is slightly larger.

The mean cloud fraction of cloudy hours in Fig. 4 is 23%. This value is low, partly due to the fact that we are detecting clouds only directly above the ceilometer and estimating the cloud fraction from this information. This value is also low because hours with a large cloud

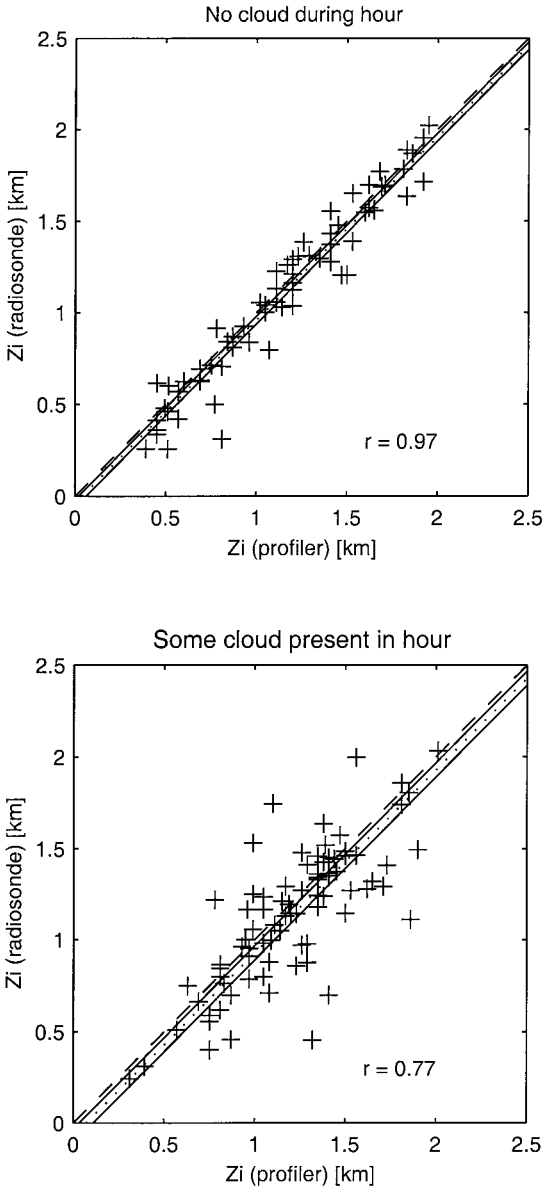

FIG. 4. Radiosonde z_i and profiler z_i stratified by the presence of cloud during the hour. For clear conditions, the mean profiler z_i = 1151 m and the mean radiosonde z_i = 1110 m. The correlation coefficient is 0.97 for 67 points. For cloudy conditions, the mean profiler z_i = 1207 m and the mean radiosonde z_i = 1136 m. The correlation coefficient is 0.77 for 83 points.

fraction are more likely to have poorly developed boundary layers or rain present and therefore to have been removed by our selection method. We are confident that the reported cloud fraction is representative of that over the area of the profiler triangle due to both the homogeneity of the terrain and the use of hour averages of hours with good agreement in boundary layer height.

The presence of clouds can move the altitude of the strongest humidity gradient higher in the entrainment zone due either to the strong effect of the sides and top of the cloud, where the humid, cloudy air is adjacent to the drier, free tropospheric air, or to increased turbulence within the cloud. Another influence on the measurements is that at each altitude the profiler samples a large volume of air for several seconds and the results are then averaged over an hour, while the radiosonde obtains a single narrow profile as it ascends. This introduces considerable scatter in the radiosonde measurements.

5. Comparison with cloud base determined from ceilometer data

Cloud-topped convective boundary layers are poorly understood. There is a continuum of behavior from cloud-free to deep convection. At the lower end of the range of cloud fraction and activity are boundary layers with fair-weather cumulus (*cumulus humilis* or *mediocris*) of roughly less than 50% coverage where the cloud layer is not deep compared to the underlying boundary layer. Under these conditions, the cloud layer can be considered to define the entrainment zone. In order to understand what profiler CBL height measurements are measuring under fair-weather cumulus conditions, we compare them with measurements from a laser ceilometer.

Cloud altitude was measured every 30 s by the ceilometer, but not all of the cloud points correspond to bases of boundary layer clouds. Wind shear may cause the cloud to tilt with altitude, so that the side of the cloud is seen, upper-level cloud (e.g., cirrus) may be present, or the measured cloud may be a passive remnant that is no longer connected to the boundary layer. In these cases the measurement should be rejected. In order to distinguish between measurements of a boundary layer cloud base and measurements of other types or parts of clouds, we incorporated surface information to obtain the LCL.

For any parcel of air, the LCL must be reached before a cloud can form. As noted by Schrieber et al. (1996), surface layer air is likely to be the most moist and buoyant and so should reach its LCL at the lowest altitude. An LCL calculated only from surface measurements neglects the effects of entrainment of air into the plume during the ascent. It is not known how much entrainment affects the thermal core, but both Crum et al. (1987) and Wilde et al. (1985) have shown that some surface air can remain undiluted in the core of a thermal rising through the mixed layer.

The LCL was calculated as described in Stull (1988). The surface measurements used for this calculation were pressure, temperature, and relative humidity, which were recorded every 30 s during the experiment. Examination of the effects of variations in each of these parameters showed that the calculation is most sensitive to relative humidity. A 5% change in relative humidity caused a variation in the calculated LCL of between 120 and 170 m in the conditions observed during this ex-

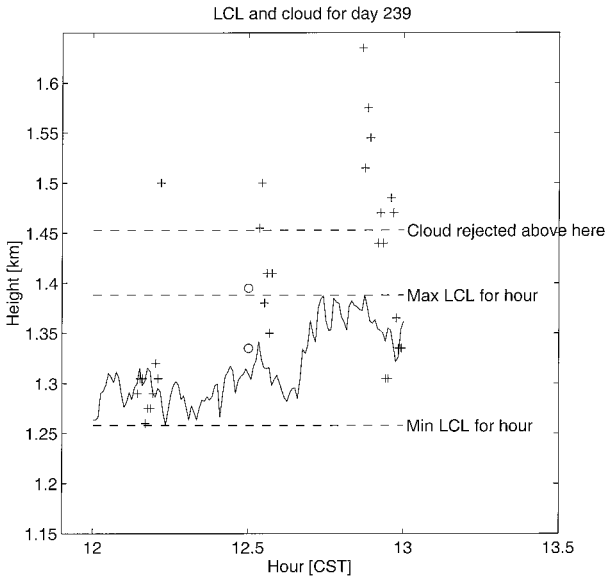

FIG. 5. Illustration of the cloud selection procedure using the calculated LCL. Measurements of cloud altitude from the ceilometer are indicated by the plus symbols. The solid line is the LCL calculated every 30 s from surface data, with dashed lines at the minimum and maximum LCL for the hour as well as at the maximum LCL plus half the variation during the hour. The top circle shows the calculated cloud altitude using all of the cloud points within the hour, while the lower circle is the cloud base calculated using only the selected cloud points.

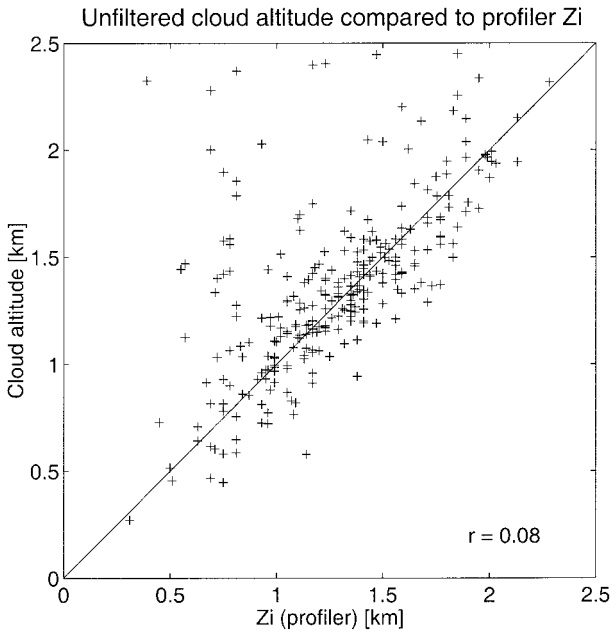

FIG. 6. Comparison of z_i found from the profiler reflectivity with the hour average cloud altitude from the ceilometer with no selection criteria applied. Cloud altitudes above 2.5 km are not shown. The mean z_i is 1255 m, and the mean cloud altitude is 1572 m. There are 311 points, and the correlation coefficient is 0.08.

periment. This uncertainty in relative humidity is of the order of the accuracy of the measurement.

The selection scheme that has been developed uses the LCL as an estimate of a reasonable range of cloud-base values. To allow for possible differences in surface characteristics, for the possibility of entrainment, and for the uncertainty in relative humidity, cloud measurements up to an altitude of the maximum LCL for the hour plus half the LCL variation during the hour were accepted. These selected cloud altitude values were then averaged, and the resulting number is called the cloud base for the hour. The procedure is illustrated in Fig. 5. Note that this method considers all of the individual cloud measurements within the hour, not just the hour-averaged cloud altitudes shown in Fig. 6. The FAO station measurements were used for the LCL calculation.

As a demonstration of the effectiveness of this fairly loose algorithm, Fig. 6 shows the average cloud altitude for each hour, as directly measured by the ceilometer (not filtered), compared to the profiler peak reflectivity. Although not shown in this figure, there are recorded hourly mean cloud altitudes up to 8 km. These large altitudes are clearly not clouds associated with boundary layer processes.

Comparison between the radar peak reflectivity and the cloud base determined using the selection criterion described (filtered) is shown in Fig. 7. The spread is partly due to the fact that cloud base depends on the characteristics of the air that forms each cloud and these

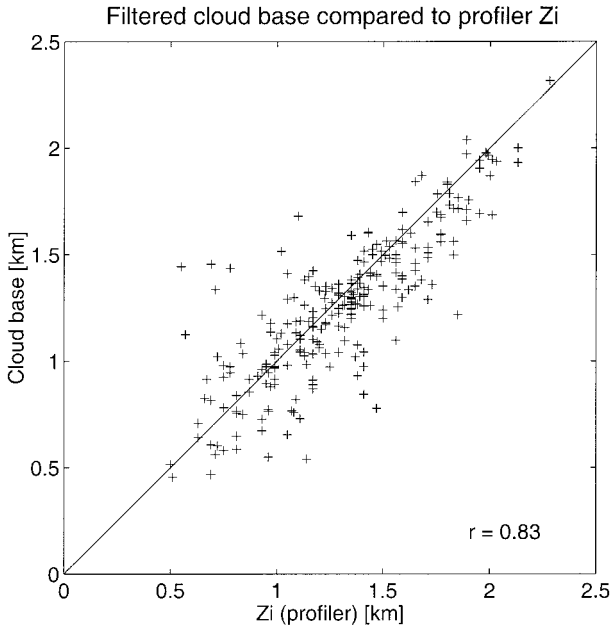

FIG. 7. Profiler z_i and cloud base as determined by the selection algorithm. Mean cloud base is 1264 m, and mean profiler z_i is 1311 m. The plot contains 258 points and has a correlation coefficient of 0.83.

can vary even over the homogeneous terrain of this experiment area. It is also seen that the profiler returns again tend to be a little higher (47 m) than the calculated cloud base. As mentioned earlier, this may be due to increased turbulence within the cloud or to the effect of sharp moisture gradients at all edges of the cloud except the bottom edge. As the air parcel rises, the relative humidity increases until at cloud base the parcel is saturated and water begins to condense out. Therefore, there is not a sharp change in the humidity at this interface. At the sides and top of the cloud, however, the surrounding air is much drier than the cloud air, and this produces a stronger radar return.

6. Richardson number comparison

A common method for determining the height of the boundary layer in computer models uses the bulk Richardson number

$$\mathrm{Ri}_b = \frac{gz\Delta\theta_v}{\overline{\theta}_v[u(z)^2 + v(z)^2]}, \quad (1)$$

where g is the gravitational acceleration, z is the current altitude AGL, θ_v is the virtual potential temperature, and u and v are the wind speed components. With the subscript s referring to a surface measurement, $\Delta\theta_v = \theta_v(z) - \theta_{vs}$, and $\overline{\theta}_v = 0.5[\theta_v(z) + \theta_{vs}]$. Surface values of u and v are assumed to be zero.

Following the method described by Pleim and Xiu (1995), we calculated Ri_b at each profiler range gate above the lower limit of 150 m since the wind velocities were found from the profiler data. The altitude at which Ri_b became greater than Pleim and Xiu's suggested critical value of 0.25 was selected as z_i. We used radiosonde profiles to calculate $\theta_v(z)$, and surface measurements for θ_{vs}.

Figure 8 shows the comparison of the calculated z_i to that measured by the profiler. There is poor agreement between the two methods, with the bulk Richardson number generally overestimating the boundary layer top compared to the profiler. Similar results are seen when z_i computed from the Richardson number is compared to that from the radiosonde measurements. This may be due to the nature of the Richardson number calculation, where the critical value chosen is not an absolute measure but can vary depending on the measurement spacing and the strength of turbulence (Stull 1988).

The results are somewhat sensitive to the choice of the critical Ri_b. Figure 8 uses $\mathrm{Ri}_b = 0.25$, which gives a mean boundary layer height from the calculation of 1457 m and a correlation coefficient of 0.62. With a critical value of $\mathrm{Ri}_b = 0$, the mean boundary layer height decreases by 73 m, and the correlation coefficient is slightly better at 0.64. A critical value of $\mathrm{Ri}_b = 1.0$, which may be more appropriate for the conditions of our experiment, raises the calculated boundary layer by 168 m, and the correlation coefficient decreases to 0.52.

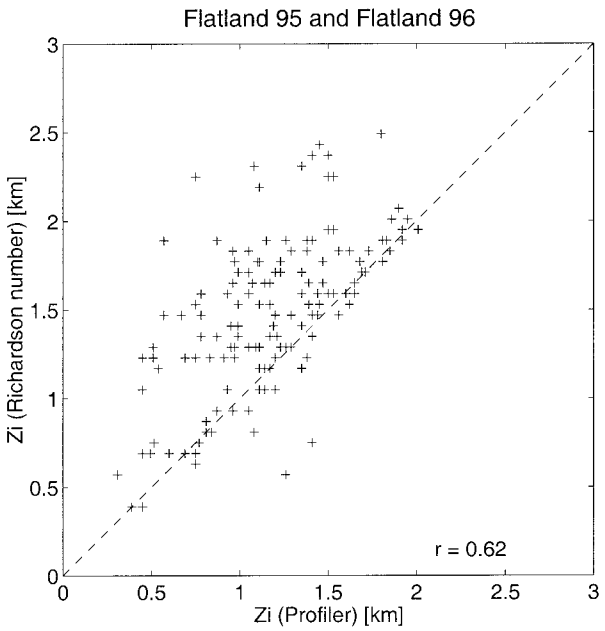

FIG. 8. Profiler z_i and z_i calculated using the bulk Richardson number. Mean z_i using Ri_b is 1457 m and mean profiler z_i is 1158 m. The plot contains 149 points and has a correlation coefficient of 0.62. The dashed line is 1:1.

7. Summary

We have shown with a large dataset that reliable estimates of the convective boundary layer height can be made from profiler data. Careful data quality control and understanding of the various observed phenomena are important. Profilers can operate reliably for long periods and provide valuable information about boundary layer evolution that is difficult to obtain from radiosondes. Another advantage is the spatial and temporal averaged nature of the measurements rather than the single narrow profile obtained by a radiosonde.

We used a ceilometer to measure cloud altitudes and mentioned that these measurements may correspond to sides of clouds, upper-level clouds, or other clouds not associated with the boundary layer. In order to obtain an estimate of the cloud base of boundary layer clouds, we have developed a method of data selection that produces very good results when compared with the boundary layer height measured by the wind profiler.

Stratification of wind-profiler data by the presence of boundary layer cloud shows a small bias in the profiler measurement when cloud is present. This may be due to strong humidity gradients at the sides and tops of the clouds or to increased turbulence within the cloud. We also see increased scatter in cloudy conditions.

A comparison of the experimental results with those from the Richardson number calculation often used in computer models shows poor agreement. We note, however, that despite this it may still be the best method available.

Acknowledgments. The Flatland Atmospheric Observatory and this project are supported by the National Science Foundation under Grant ATM-9419638. The Integrated Sounding Systems (ISS) were provided by the National Center for Atmospheric Research and Sounding Systems Facility. The FAO and Monticello Road sites were provided by the University of Illinois Department of Electrical Engineering. Stanley Henson of the University of Illinois operates and maintains the FAO.

Mention of a commercial company or product does not constitute an endorsement by NOAA/ERL. Use of information from this publication concerning proprietary products or the tests of such products for publicity or advertising purposes is not authorized.

REFERENCES

Angevine, W. M., A. B. White, and S. K. Avery, 1994: Boundary layer depth and entrainment zone characterization with a boundary layer profiler. *Bound.-Layer Meteor.,* **68,** 375–385.

——, A. W. Grimsdell, J. M. Warnock, W. L. Clark, and A. C. Delany, 1998: The Flatland Boundary Layer Experiments. *Bull. Amer. Meteor. Soc.,* **79,** 419–431.

Carter, D. A., K. S. Gage, W. L. Ecklund, W. M. Angevine, P. E. Johnston, A. C. Riddle, J. Wilson, and C. R. Williams, 1995: Developments in UHF lower tropospheric wind profiling at NOAA's Aeronomy Laboratory. *Radio Sci.,* **30,** 977–1001.

Clark, W. L., J. M. Warnock, T. E. VanZandt, and K. S. Gage, 1995: Scattering from clear air, precipitation and biological targets: Multiple frequency profiler studies. Preprints, *27th Conf. on Radar Meteorology,* Vail, CO, Amer. Meteor. Soc., 281–283.

Crum, T. D., R. B. Stull, and E. W. Eloranta, 1987: Coincident lidar and aircraft observations of entrainment into thermals and mixed layers. *J. Climate Appl. Meteor.,* **26,** 774–788.

Donaldson, N., W. O. J. Brown, and R. R. Rogers, 1997: Radar observations of the planetary boundary layer during MERMOZ. Preprints, *12th Symp. on Boundary Layers and Turbulence,* Vancouver, BC, Canada, Amer. Meteor. Soc., 421–424.

Ecklund, W. L., D. A. Carter, and B. B. Balsley, 1988: A UHF wind profiler for the boundary layer: Brief description and initial results. *J. Atmos. Oceanic Technol.,* **5,** 432–441.

Grossman, R. L., and N. Gamage, 1995: Moisture flux and mixing processes in the daytime continental convective boundary layer. *J. Geophys. Res.,* **100** (D12), 25 665–25 674.

Merritt, D. A., 1995: A statistical averaging method for wind profiler Doppler spectra. *J. Atmos. Oceanic Technol.,* **12,** 985–995.

Pleim, J. E., and A. Xiu, 1995: Development and testing of a surface flux and planetary boundary layer model for application in mesoscale models. *J. Appl. Meteor.,* **34,** 16–32.

Schrieber, K., R. Stull, and Q. Zhang, 1996: Distributions of surface-layer buoyancy versus lifting condensation level over a heterogeneous land surface. *J. Atmos. Sci.,* **53,** 1086–1107.

Stull, R. B., 1988: *An Introduction to Boundary Layer Meteorology.* Kluwer Academic, 666 pp.

Trainer, M., B. A. Ridley, M. P. Buhr, G. Kok, J. Walega, G. Hübler, D. D. Parrish, and F. C. Fehsenfeld, 1995: Regional ozone and urban plumes in the southeastern United States: Birmingham, a case study. *J. Geophys. Res.,* **100,** 18 823–18 834.

White, A. B., 1997: Horizontal variation in mixing depth observed during the 1995 Southern Oxidants Study. Preprints, *12th Symp. on Boundary Layers and Turbulence,* Vancouver, BC, Canada, Amer. Meteor. Soc., 38–41.

——, C. W. Fairall, and D. W. Thomson, 1991: Radar observations of humidity variability in and above the marine atmospheric boundary layer. *J. Atmos. Oceanic Technol.,* **8,** 639–658.

Wilde, N. P., R. B. Stull, and E. W. Eloranta, 1985: The LCL zone and cumulus onset. *J. Climate Appl. Meteor.,* **24,** 640–657.